Scientific Research Publishing

Open Journal of Geology, 2025, 15(8), 503-523
https://www.scirp.org/journal/ojg
ISSN Online: 2161-7589
ISSN Print: 2161-7570

Petrographic and Geochemical Characterization of Dolerites East of Léré in Mayo Kebbi (South-West of Chad): Geodynamic Implication

Klamadji Moussa Ngarena[1*], Moussa Ali Baradine[2], Tékoum Léontine[2], Moussa Abderamane[2], Baïssemia Ronang Gustave[1], Djerossem Nenadji Felix[3], Courage Gabvourta[4]

[1]Department of Mining and Geology Engineering, Faculty of Earth and Life Sciences, University of Pala, Pala, Chad
[2]Department of Geology, Faculty of Exact and Applied Sciences, University of N'Djamena, N'Djamena, Chad
[3]Department of Mines, New and Renewable Energies, National Higher Institute of the Sahara and Sahel, Iriba, Chad
[4]Department of Earth Sciences, University of Dschang, Dschang, Cameroon
Email: *klamadjimoussa@yahoo.fr

How to cite this paper: Ngarena, K.M., Baradine, M.A., Léontine, T., Abderamane, M., Gustave, B.R., Felix, D.N. and Gabvourta, C. (2025) Petrographic and Geochemical Characterization of Dolerites East of Léré in Mayo Kebbi (South-West of Chad): Geodynamic Implication. *Open Journal of Geology*, **15**, 503-523.
https://doi.org/10.4236/ojg.2025.158024

Received: March 21, 2025
Accepted: August 25, 2025
Published: August 28, 2025

Abstract

The study area located in Mayo Kebbi belongs to the Northern domain of the Pan-African Range of Central Africa. This work is a contribution to the geological and geochemical study of dolerites in Mayo Kebbi. The main objective of our study is to carry out petrological and geochemical studies of dolerites around Léré and to determine their geodynamic context of emplacement. The methodology of this study is based on an integrated approach combining field work, petrographic and geochemical analyses. The field work revealed that dolerite dykes outcrop in the form of balls and blocks of light to dark gray shades cutting the Pan-African basement. These dolerite dykes have thicknesses varying from 5 to 20 m and lengths of the order of decameters to kilometers; and show main orientations of E-W and N-S. The petrographic study identified three facies: pyrite and basement enclave dolerites, pyrite and calcite dolerites, and amphibole and pyroxene dolerites, including doleritic and ophitic textures. The primary mineral assemblage consists of plagioclases, pyroxenes, oxides, hornblende, apatite and biotite, sometimes pyrite and calcite. Whole rock geochemical analyses using ICP-MS and ICP-AES methods determined the compositions of different facies of the dolerites: pyrite and basement enclave dolerites and pyrite and calcite dolerites are basic to intermediate hypovolcanic rocks (SiO_2: 45.2% - 58.2%), with alumina (Al_2O_3: 14.65% - 17.85%). Amphibole and pyroxene dolerites (SiO_2: 60.3% - 65.1%) are classified in the acid rock field. Transition element concentrations vary (Ni: 4 - 68 ppm and V: 73 - 322 ppm) showing a fractionation of iron-titanium oxides. The geodynamic context of emplacement of these rocks is typical of late to post-orogenic (compressive to distensive) to orogenic (compressive) intracon-

tinental zones.

Keywords

Dolerites, Léré, Pan-African Chain, Petrography, Geodynamics, Geochemistry

1. Introduction

Intrusive magmatism generally exploits synchronous fracturing systems and can also follow regenerated pre-existing systems that exhibit network organizations [1]. Doleritic magmatic intrusions are designated under two groups in Central Africa: extensional basin dolerites and continental tholeiite dolerites. Extensional basin dolerites have been identified in Anambra, Nigeria [2] and in northern Cameroon, in the Mayo Oulo-Léré and Babouri-Figuil regions [3]. Large Igneous Provinces (LIPs) result in the eruption of large quantities of basaltic magmas in a very short geological time [4]. These large volcanic provinces representing vast areas on Earth are made up essentially of mafic rocks of tholeiitic nature which appear in the form of flows, sills and dykes [5] [6]. The emplacement of basic to intermediate intrusions, which very often outcrop in the form of dykes and sills, is considered a direct consequence of the tectonic events that affected the Pan-African basement [7] [8]. Basalt or dolerite dykes of bimodal composition (basaltic to ultrabasaltic) have been studied in the African cratonic domains and the Pan-African Range domain [9] [10]. In the Léré region of southwest Chad, hypovolcanic formations cut the Pan-African basement. These basic magmatic formations outcrop in the form of dykes cutting the Pan-African basement. This study focuses on the dolerites of the Pan-African basement of eastern Léré. The emplacement of basic to intermediate intrusions, which very often outcrop in the form of dykes and sills, is considered to be a direct consequence of the tectonic events that affected the Pan-African basement [7] [8]. Basalt or dolerite dykes of bimodal composition (basaltic to ultrabasaltic) have been studied in the African cratonic domains and the Pan-African Range domain [9] [10]. The work on the dolerites of Léré and Figuil is based on the petrographic, mineralogical and geochemical aspects [3] [11]-[14]. The petrographic and geochemical characteristics of these doleritic intrusions have allowed us to specify the geodynamic context of their emplacement. The dolerites of the Pan-African basement around Léré have not benefited from in-depth petrographic and geochemical studies. The main objective is to carry out petrological and geochemical studies of the dolerites of the Pan-African basement. The specific objectives of this work are: 1) to gather as much information as possible on the dolerites of the Pan-African basement around Léré; 2) to specify the type and nature of these rocks by focusing on a microscopic study and geochemical data; and 3) to determine the geodynamic context of the emplacement of these dolerites of the Pan-African basement. The approach of this study is therefore perfectly suited to provide new data on the geodynamic context of dyke

emplacement and magmatic activity in the study area.

2. Geological Framework

Chad is part of a vast domain called the Mobile Zone or the Central African Pan-African Range (CPAC) [15]. The Central African Mobile Zone extends from the northern edge of the Congo Craton to eastern Nigeria, encompassing Cameroon, Chad, and the Central African Republic. It continues eastward to Sudan and Uganda [16], and westward to Brazil (São Francisco Craton, Trans-Amazonian Belt) [17] [18]. The Mayo Kebbi, located in southwest Chad, where the study area is located, is a geologically rich and complex region (**Figure 1**). This region is characterized by a variety of Precambrian formations that testify to the geological evolution of the Pan-African Range [11]-[13] [19]-[23]. The crystalline basement of the Mayo Kebbi consists of several lithotectonic formations, which are distinguished by their composition and geological history. The main formations identified in this region include: 1) greenstone belts, 2) the Mayo-Kebbi batholith, and 3) post-tectonic intrusions. The Mayo Kebbi bedrock, which extends from Cameroon to southwest Chad, is interpreted as a Neoproterozoic middle arc, stabilized around 640 Ma [24]. The basement of the Mayo Kebbi region consists of granites and gneisses, which were folded NNE-SSW by the Pan-African orogeny and characterized by the presence of N-S to NNE-SSW oriented foliations carrying an E-W stretching lineation with dips greater than 50˚ to the West [24]. In the Léré region, the geological contacts are studied between the Zalbi metavolcano-sedimentary series and the Mafic and Intermediate Complex, on the one hand, and between the latter and the Léré batholith, on the other hand. The metavolcano-sedimentary series is mainly composed of chloritoschists, with intercalations of talcschists and some rare serpentinites. The rocks of the Mafic and Intermediate Complex, represented by gabbros, gabbro-diorites and quartz diorites. The presence of vein appendages from the Léré batholith within the Mafic and Intermediate

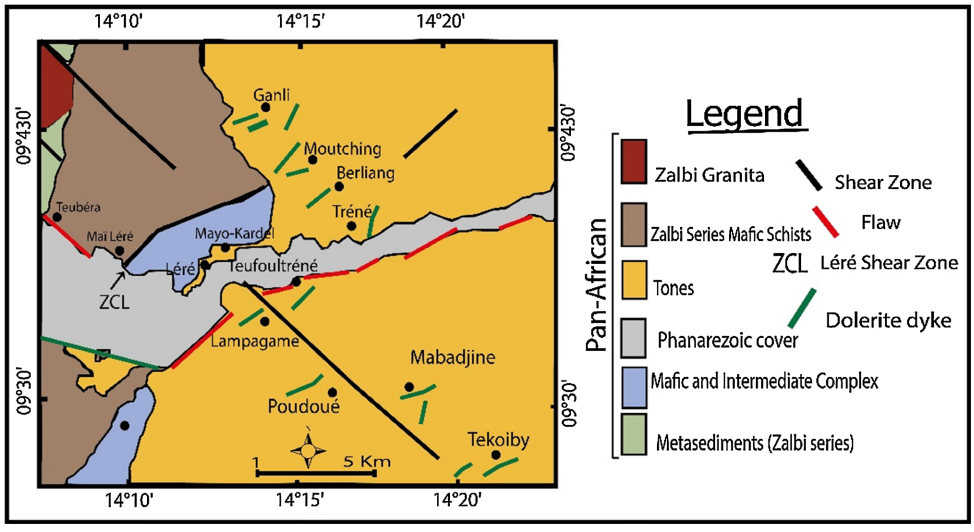

Figure 1. Geological and structural map of the study area [22].

Complex indicates an intrusive character of the batholith in the latter, as suggested by [22] (**Figure 1**).

The study area is part of the CPAC, dolerites outcrop on the Pan-African basement. These dolerites are present in the form of dykes, they are abundant in variable directions and of fairly significant extension, outcropping within the formations of middle to upper Proterozoic age, covered by sediments of lower Cretaceous age [25]. The difference in incompatible elements (REE: La, Nd and Ce) between the two groups of dolerites is explained by the degree of partial fusion of the same source which becomes more important over time. The mode of emplacement of these two groups of dolerites in the Pan-African basement seems to be a direct consequence of the tectonic events which affected these regions [11]-[13].

3. Material and Methods

3.1. Material

Ten (10) fresh and representative dolerite samples were selected based on their health and degree of alteration for petrographic and geochemical studies. Sample was carefully cleaned and then sawn into two rock sugar cubes. Ten (10) rock cubes were ground (pretreatment) at the laboratory of the Ministry of Mines and Geology of Chad and then sent to the ALS laboratory (South Africa) for geochemical analyses. The other ten (10) were sent to the thin-section laboratory of the Department of Earth Sciences at the University of Yaoundé I (Cameroon) for thin-section preparation.

3.2. Methods

Before proceeding with the analyses: 0.2 g of powder from each sample was first melted with 1.5 g of Lithium meta-borate/tetra borate ($LiBO_2/Li_2B_4O_7$) and then dissolved in 100 mm^3 of 5% dilute nitric acid. The analytical uncertainties vary from 0.1% to 0.04% for major elements; from 0.1% to 0.5% for trace elements; and from 0.01 to 0.5 ppm for rare earths. The remaining trace elements were analyzed by ICP-MME. Loss on ignition or LOI (Loss on ignition) for ICP-MS and ICP-AES (Inductively Coupled Plasma Atomic Emission Spectrometry) analyses is also known as calcination. Its determination is done by heating the powders to the point that they release all their water bound to the particles.

Once in solution, the samples were analyzed by Inductively Coupled Plasma-Atomic Emission Spectrometry (ICP-AES). The prepared samples were mixed with the $LiBO_2/Li_2B_4O_7$ flow. The samples were dissolved under a Teflon bomb pressure, using a 1:1 mixture of HF and $HClO_4$ at 180˚C, and then taken up in an HNO_3 solution with an international In-Re standard. After dissolution in HF-$HClO_4$, the samples were taken into a mixture of HNO_3, HCl and HF and diluted. These solutions were measured within 24 hours of dilution to prevent HFSE absorption. For major elements, a comprehensive major element analysis was performed by combining several methods in a single package. This package combines the entire whole-rock analysis package (ME-ICP06) in addition to carbon and sul-

fur, which are analyzed using a combustion furnace (ME-IR08). The elements SiO_2, Al_2O_3, Fe_2O_3, CaO, MgO, Na_2O, K_2O, Cr_2O_3, TiO_2, MnO, P_2O_5, SrO, and BaO were analyzed by ICP-AES.

4. Results

4.1. Petrography

The dolerite dykes covered by this study are rarely more than twenty meters thick and vary in length. The petrographic study revealed three dolerite facies based on color and mineralogical composition. These are pyrite and basement enclave dolerites rich in alkali feldspars, pyrite and calcite dolerites, and amphibole and pyroxene dolerites, with doleritic, granophyre intergranular, and ophitic textures respectively. The primary mineralogical assemblage of these rocks is often completely or partially transformed. Plagioclase and pyroxene are the dominant mineral phases.

4.1.1. Pyrite Dolerites and Basement Enclaves Rich in Alkali Feldspars

The pyrite and enclave dolerites of the Léré basement are observed at Berliang, Ganli, Tréné and Moutching. They crop out in the form of rectilinear dykes with ENE-WSW, N-S directions in Berliang; ENE-WSW, NNE-SSW to Ganli; from N-S to Tréné; from ENE-WSW, NNE-SSW to Moutching. These dolerite dikes form centimeter-sized balls (20 to 60 cm) and metric blocks (1 to 2 m) (**Figures 2(a)-(e)**). They have powers varying from 7 to 18m over metric to kilometric lengths. Under the microscope, dolerites have a doleritic texture. They are made up of phenocrysts and microcrystals of clinopyroxene oxides, alkali feldspars, plagioclase, amphibole, iron oxides. Plagioclases are more abundant and appear in the form of laths and often in microlites and generally automorphic phenocrysts. Secondary minerals such as microcline, epidote and chlorite were also observed in the thin sections (**Figures 2(b)-(f)**).

4.1.2. Pyrite and Calcite Dolerites

The pyrite and calcite dolerites crop out in the form of dikes made up of metric blocks (around 1 m) and centimeter-sized balls (20 to 50 cm) intersecting the base following the NE-SW to ENE-WSW direction at Tefoultréné and ENE-WSW to N-S to Lampagame (**Figure 2(c)**). These dark gray dolerite dykes have thicknesses varying from 7 to 15 m over kilometer lengths. Contact with the base is clear. At the fresh break, the rocks are hard, dark, massive, with a porphyry microlitic structure and present a brown weathering patina (2 mm). The matrix is composed of feldspar, pyroxene, opaque crystals and pyrite crystals (**Figure 2(d)**). Under the microscope, the dolerites show an intergranular to granophyre texture. These dolerites are composed of phenocrysts of plagioclase, clinopyroxene, iron oxide, alkali feldspars, calcite with corrosion gulfs and their microcrystals, thus plagioclase microlites are observed. Secondary minerals observed in the thin sections are epidote, pyrite and chlorite (**Figure 2(d)**).

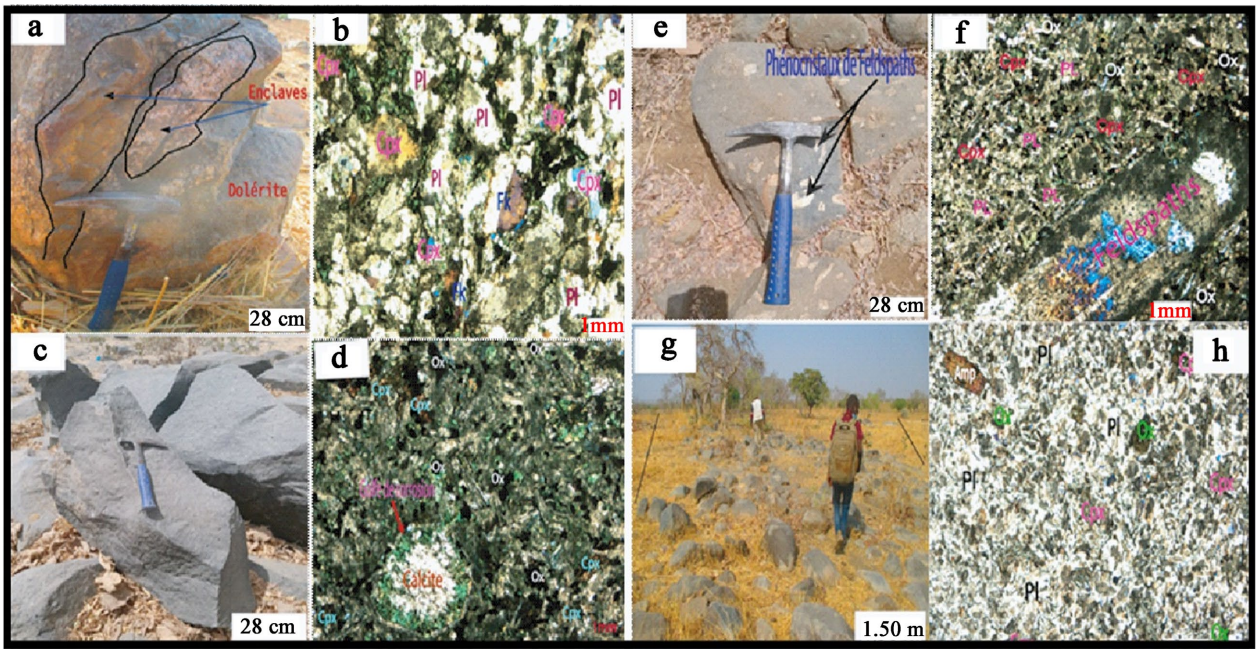

Figure 2. Some samples and photomicrograph showing structural and textural characteristics of dolerites. (a) Representative sample of pyrite and enclave dolerites taken from Berliang; (b) Crystals of plagioclase, clinopyroxene and alkali feldspars in the doleritic texture in LPA(BM1); (c) Outcrop in the form of blocks of dolerite dykes with pyrite and calcite at Lampagame; (d) Calcite crystals with corrosion gulfs in dolerite with pyrite and calcite in LPA; (e) sample with porphyritic dolerite structure of dolerite with pyrite and enclaves rich in alkali feldspars from eastern Léré; (f) Classic doleritic texture of dark dolerite with pyrite and alkali feldspars in LPA (BeM3); (g) Outcrop of a dolerite dyke in the form of balls and blocks at Léré; (h) Crystals of plagioclase, clinopyroxene, oxide and amphibole in the ophitic texture in LPA (MaM4).

4.1.3. Amphibole and Pyroxene Dolerites

Amphibole and pyroxene dolerites crop out in the form of rectilinear dikes made up of centimetric (15 to 60 cm) to metric (more than 1 m in diameter) balls and blocks. These dykes vary in size from 5 to 15m over a few kilometers in length and intersect the basement following the ENE-WSW direction at Tekoiby; N-S to Mabadjin and from ENE-WSW to Poudoué. The rocks are hard, freshly broken, massive, gray and with a doleritic structure. The rocks are made up of crystals of alkali feldspars, pyroxene, oxides and fine, elongated microcrystals. They present a thin (less than 3 mm) brown to reddish weathering patina (**Figure 2(g)**). Under the microscope, dolerites have an ophitic texture typical of dolerites. They are made up of clinopyroxene phenocrysts surrounding the plagioclase laths. Phenocrysts of clinopyroxene, plagioclase, amphibole, and oxides were observed. These phenocrysts are distributed in a matrix composed of plagioclase microlites, clinopyroxene and iron-titanium oxide microcrystals. Secondary minerals such as iron-titanite oxides, apatite and chlorite were observed in some sections of the phenocrysts in the thin sections (**Figure 2(h)**).

4.2. Geochemical Characterization

Chemical analyses on whole rocks are carried out on the different petrographic types representative of the dolerites of the surroundings of Léré. The results are

compiled in Table 1. The mafic hypovolcanic rocks are rocks of basaltic and homogeneous composition (45.2% SiO_2 65.1%; 4.24 Fe_2O_3 15.85%; 2.05 MgO 4.89%; 0.58 TiO_2 3.47%; 14.65 Al_2O_3 17.85 and 4.5 Na_2O + K_2O 7.5). Such a composition, typical of tholeiitic magmas [26] [27], reflects a crystallization of oxides as suggested by the textural relationships. The behavior of trace and major elements is consistent with the crystallization of clinopyroxenes and plagioclases which are the most important mineral phase. In detail, the progressive decrease in TiO_2 and Fe_2O_3 contents is related to the continuous fractionation of ferro-titanium oxides. The pyrite-enclave basement dolerites and the pyrite-calcite dolerites show varied geochemical characteristics indicating their classification as basic to intermediate (SiO_2: 45.2% - 58.2% and Al_2O_3: 14.65% - 17.85%). The amphibole-pyroxene dolerites show higher SiO_2 contents, between 60.3% and 65.1%, classifying them as acidic rocks. The concentrations of transition elements, such as nickel (4 to 68 ppm) and vanadium (73 to 322 ppm), suggest some degree of fractionation of the iron-titanium oxides.

Table 1. Whole rock analyzes of dolerite dikes outcropping on the basement.

(%)	TrM1	BM2	MoM1	GaM1	GaM3	TtM1	LaM1	TEM2	MaM4	POM1
SiO_2	45.4	58.2	45.2	49.6	47.4	45.9	45	65.1	63.3	60.3
TiO_2	2.57	1.14	3.47	2.8	2	2.39	2.39	0.58	0.61	0.97
Al_2O_3	15.6	16.35	14.65	14.95	17.85	15.9	15.6	15.8	15.75	15.65
Fe_2O_3	14.05	7.46	15.85	13.45	11.65	13.3	13.7	4.24	4.44	5.77
MnO	0.17	0.13	0.19	0.17	0.15	0.17	0.16	0.07	0.09	0.1
MgO	4.65	2.05	4.45	3.27	4.51	5.1	4.89	2.83	2.92	3.65
CaO	7.33	5.51	7.05	5.63	7.14	7.21	7.09	3.69	3.86	4.04
Na_2O	3.58	4.23	2.85	4.13	3.59	3.2	3.59	4.77	4.55	4.58
K_2O	1.2	1.52	2.12	2.37	1.4	1.3	1.32	2.73	2.66	2.71
P_2O_5	0.52	0.41	0.69	1	0.35	0.44	0.45	0.16	0.16	0.21
Cr_2CO_3	0.005	0.011	0.005	0.004	0.006	0.006	0.004	0.036	0.033	0.025
SrO	0.06	0.05	0.05	0.07	0.06	0.06	0.07	0.06	0.08	0.05
BaO	0.04	0.06	0.08	0.13	0.08	0.06	0.05	0.07	0.07	0.06
LOI(PF)	5.96	1.98	2.03	3.07	3.35	4.15	5.3	1.56	1.42	1.86
Total	**101.14**	**99.1**	**98.69**	**100.64**	**99.54**	**99.19**	**99.61**	**101.7**	**99.94**	**99.98**
ppm										
Sc	16	13	18	13	15	16	16	8	8	10
V	208	101	322	169	186	203	210	73	81	121
Co	44	15	50	31	41	49	44	13	13	19
Ni	45	4	37	10	52	61	53	33	34	68
Ga	24.6	22.5	27.2	26.9	23.9	24.8	25.5	22.9	24.1	25.1

Continued

Rb	23	21.2	43.7	36	39	19.4	19.6	66.7	68.7	76.6
Sr	563	486	575	655	611	658	682	565	761	509
Y	28.7	36	38	42.7	22.8	26.1	27.3	9.6	9	11.8
Zr	250	433	330	422	200	225	232	146	148	166
Nb	25.3	13.55	35.6	42.6	18.05	22.4	22.4	6.91	7.24	8.95
Sn	2.2	1.3	2.6	2.7	1.2	1.8	1.9	1.1	1.7	2.3
Cs	2.57	0.5	1.78	1.38	1.17	2.44	0.96	1.28	1.57	2.8
Ba	390	550	768	1160	670	531	462	593	594	556
La	29.1	33.7	43.1	55.8	19.8	25.1	26.3	23.8	24.1	26.4
Ce	66.1	71.9	97.5	124.5	44.5	58	60.2	45.9	47.8	52.7
Pr	8.44	8.63	12.6	16.3	5.94	7.6	7.67	5.4	5.51	6.2
Nd	36.2	37	52.3	67.7	25.2	32.5	33.9	20.3	20.4	23
Sm	8.08	7.24	10.75	13.7	5.64	7.27	7.78	3.42	3.88	4.75
Eu	2.36	2.16	3.01	3.75	1.87	1.99	2.28	1.08	0.99	1.17
Gd	7.92	8.1	10.3	11.7	5.34	6.56	7.15	2.49	2.77	3.32
Tb	1.09	1.24	1.32	1.64	0.84	0.91	0.99	0.32	0.37	0.42
Dy	6.02	7.1	8.05	9.1	4.85	5.5	5.77	1.8	1.82	2.29
Ho	1.08	1.42	1.34	1.63	0.89	0.98	1.04	0.35	0.31	0.5
Er	2.96	4.03	3.6	3.92	2.25	2.49	2.86	1.05	0.9	1.27
Tm	0.4	0.51	0.49	0.55	0.34	0.31	0.4	0.13	0.12	0.16
Yb	2.3	3.21	2.7	2.86	1.76	2.02	2.13	0.73	0.99	0.95
Lu	0.3	0.52	0.45	0.44	0.33	0.31	0.34	0.14	0.14	0.19
Hf	6.24	9.45	7.37	10.3	4.95	5.33	5.73	4.16	4.07	4.22
Ta	1.2	0.7	1.7	2.3	1	0.9	1	0.5	0.5	0.6
W	0.7	<0.5	0.6	0.5	<0.5	0.9	0.5	<0.5	0.6	0.7
Th	2.27	4.03	3.01	3.8	1.63	1.95	2.01	9.77	9.33	11.75
U	0.58	0.59	0.64	0.93	0.44	0.52	0.55	3.94	3.94	4.58

In the TAS classification diagram, the sum of alkali (Na_2O+ K_2O) versus SiO_2 [28] (**Figure 3**) of igneous rocks reveals that some studied dolerites fall into the basalt, trachy-basalt field except amphibole and pyroxene dolerites which are plotted in trachy-andesite and trachyte domains. Only one sample of pyrite and basement enclave dolerites is found in the andesite range.

The AFM diagram [29] (**Figure 4**) shows that the studied dolerite samples are distributed along a boundary line. The pyrite-basement enclave dolerite facies and the pyrite-calcite dolerites are found in the area corresponding to the tholeiitic series, indicating that they are rich in FeOt and poor in MgO. This suggests an

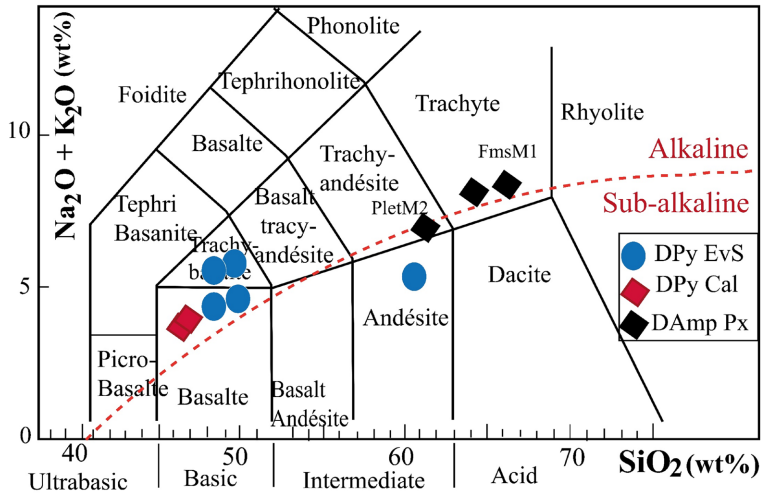

Figure 3. TAS classification diagram ($Na_2O + K_2O$ versus SiO_2) [28]. Figured blue: dolerites with pyrite and basement enclave (DPyEvS); Figured red: dolerites with pyrite and calcite (DPyCal) and Figured black: dolerites with amphibole and pyroxene (DAmpPx).

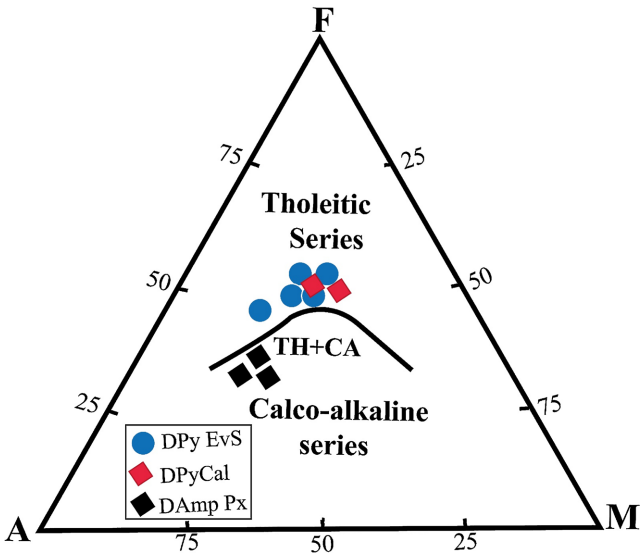

Figure 4. Position of the dolerites from eastern Léré in the AFM diagram [26], the red curve indicates the limit of the tholeiitic and calc-alkaline domains.

origin in environments such as oceanic ridges. The amphibole-pyroxene dolerite facies are located in the area of the calc-alkaline series, where they show higher $Na_2O + K_2O$ contents and reduced FeOt levels. They suggest a formation in subduction environments, typical of volcanic arcs.

Harker diagrams highlight the evolution of major elements expressed as weight percentage of oxides as a function of SiO_2. Harker diagrams for major elements show a decreasing trend for TiO_2, Fe_2O_3, MnO, MgO, CaO, and P_2O_5 as SiO_2 increases. Al_2O_3 shows a constant profile. This suggests a fractionation of mafic minerals such as clinopyroxenes and opaques. For K_2O, Na_2O, and Cr_2CO_3, they show an increasing trend with increasing SiO_2 (**Figure 5**).

Chondrite-normalized rare earth element spectra [30] (**Figure 6(a)**) of dolerites

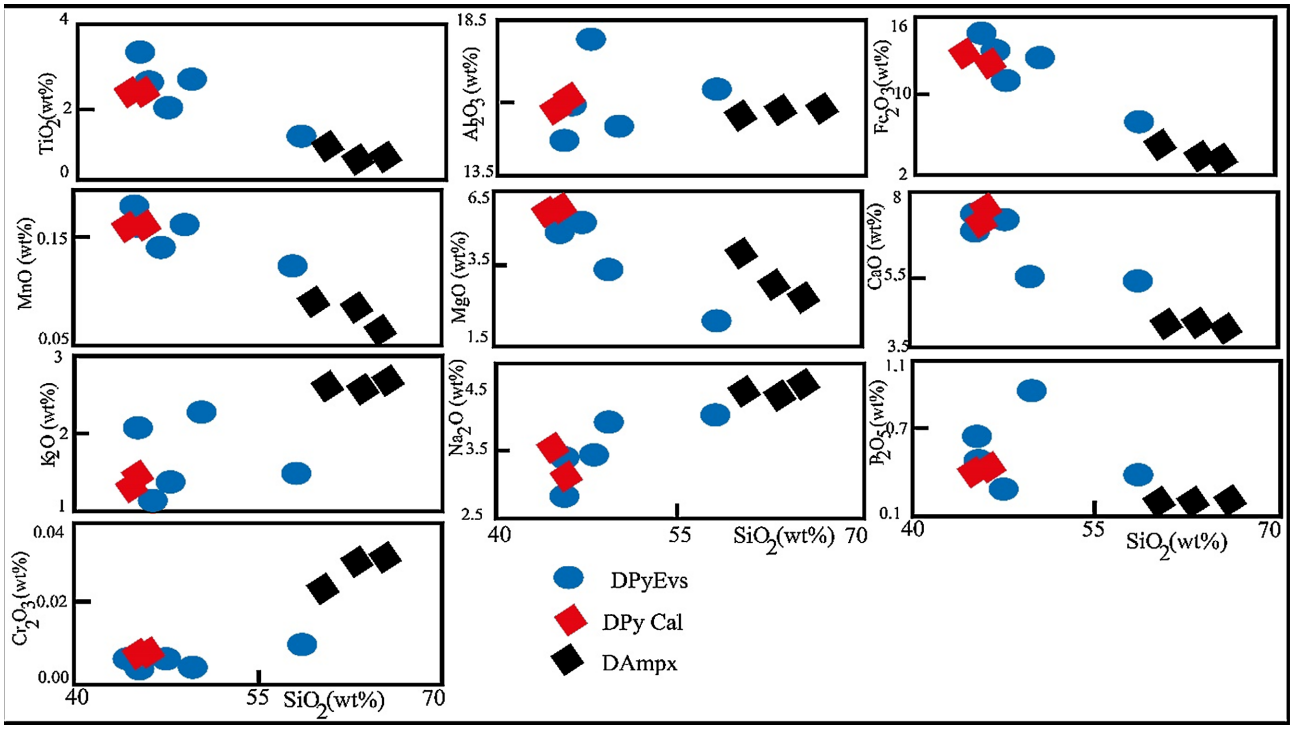

Figure 5. Harker diagrams of evolutions of major elements as a function of SiO_2 of mafic magmatic rocks in the study area. Figured blue: dolerites with pyrite and basement enclave (DPyEvS); Figured red: dolerites with pyrite and calcite (DPyCal) and Figured black: dolerites with amphibole and pyroxene (DAmpPx).

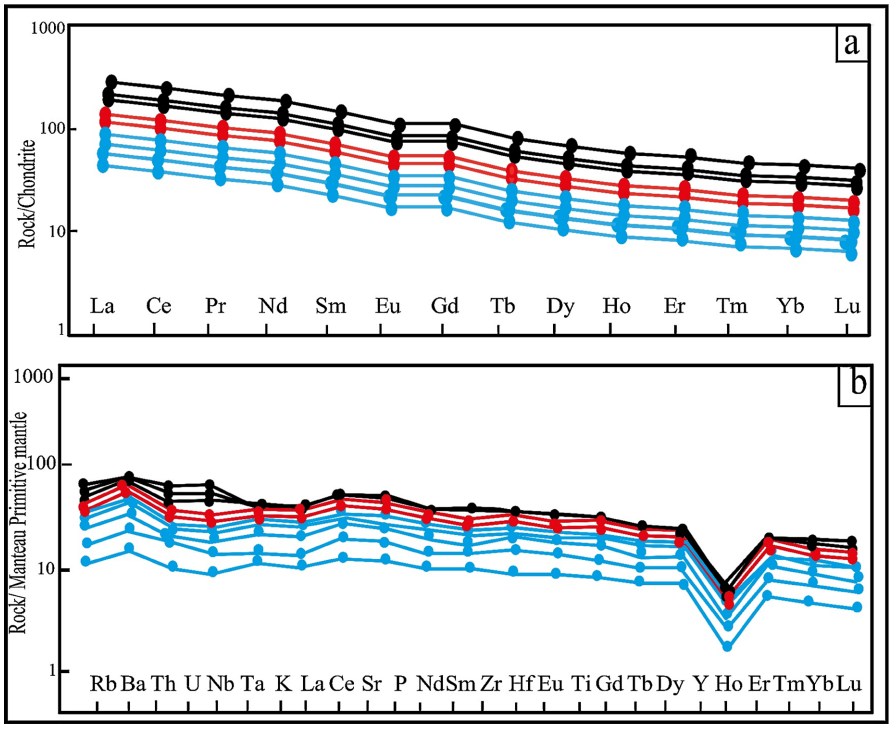

Figure 6. Rare earth spectra and multi-element diagrams of basement dolerites east of Léré normalized to chondrites [30] and primitive mantle [30]. (a) Multi-element spectra of dolerites from eastern Léré; (b) Rare earth spectra of rocks studied. Figured blue: dolerites with pyrite and basement enclave (DPyEvS); Figured red: dolerites with pyrite and calcite (DPyCal) and Figured black: dolerites with amphibole and pyroxene (DAmpPx).

show enrichment in light rare earth elements (LREE) relative to heavy rare earth elements (HREE), with a slight negative Eu anomaly. Multi-element trace element spectra of dolerites normalized to the primitive mantle of [30] (**Figure 6(b)**) are characterized by negative anomalies in Th, Ta, Nd, and Tb, positive anomalies in Ba, Nb, La, Zr, and enrichment in incompatible LILE elements (Rb, Ba, Th) relative to incompatible HFSE elements (Dy, Y, Yb). These features are associated with calc-alkaline magmas formed in subduction zones. They result from the enrichment of the source mantle of these magmas by fluids.

4.3. Discussion

Petrographic and geochemical data are used in this part of the work to categorize, determine the nature and geodynamic context and the origin of the rocks studied.

4.3.1. Macroscopic Characteristics

Field observations have highlighted the presence of three (3) facies, namely, pyrite and basement enclave dolerites, pyrite and calcite dolerites and dark grey amphibole and pyroxene dolerites intersecting the Pan-African basement aged 640 Ma [24] to 630 ± 1 Ma [22], this outcrop mode, later than the Pan-African basement, shows the post-tectonic character. The absence of macroscopic deformation structures may reflect their post-tectonic character. The existence of weathering patina on the dolerites is the result of water percolation through various fractures. The dolerite dykes of the study area and those of Léré and Figuil [11]-[13] are wider than the basaltic dykes of Bangangté, Dschang and Manjo (0.2 to 1.2 m wide) [31] and the doleritic dykes of Likok (10 to 15 m wide) [32].

Dyke widths appear to be related to crustal extension. Dyke size may also provide some information about the emplacement mechanism. [33] suggested that the primitive magma flows that generated continental dykes with widths greater than 3 m would be turbulent rather than laminar. Turbulent magma flows feeding wide dykes may have promoted some crustal contamination, because the magma rising to the surface would have eroded the dyke walls. In contrast, the laminar flow of the thin Biden [34], Bangangté, Dschang, and Manjo [31] dykes could not have promoted crustal contamination.

4.3.2. Microscopic Characteristics

Microscopic observations of the studied rocks have highlighted the different textures such as doleritic, intergranular granophyre, and ophitic textures. Textural relationships may suggest two phases of magma crystallization with the first phase characterized by the crystallization of ferromagnesian mineral phenocrysts (such as clinopyroxene, amphibole, and opaques) and the second phase marked by the crystallization of titanite microcrystals and microliths. These textural relationships imply two modes of mineral growth: simultaneous crystallization and early crystallization of minerals. For example, ophitic texture is the mineral growth mode due to simultaneous crystallization of ferromagnesian crystals (clinopyroxene) and alkali feldspars or plagioclases, while subophitic texture is the mineral

growth mode suggesting early crystallization of ferromagnesian minerals and late crystallization of feldspars.

Following hydrothermal alteration accompanying the emplacement of these intrusions, the primary minerals of these magmatic rocks underwent more or less significant and very heterogeneous post-magmatic transformations, both at the mineral scale and that of the different magmatic facies. Thus, a secondary paragenesis with chlorite, albite, sphene, epidote, sericite, calcite, pyrite and quartz developed, at the expense of the primary minerals. The established order of crystallization is as follows: titanites would have crystallized first, clinopyroxene crystals second, amphiboles, biotite and finally those of plagioclases and alkali feldspars. Automorphic titanites can result from the alteration of clinopyroxene phenocrysts and xenomorphic titanites are frequently grouped into two or more individuals by the edges.

4.3.3. Geochemical Characteristics

1) Rock Petrogenesis

Undersaturated alkaline magmas rich in volatile elements are markers of the important role of fluids in the mantle and of fluid-rock and magma-rock interactions, key processes for understanding convective mantle dynamics and asthenosphere-lithosphere interactions in the intracontinental domain [35]. If we consider the possible variations in all the characteristics (chemical and mineralogical composition) of a mantle source and the melting conditions (temperature, pressure, melting rate), it becomes theoretically possible to design a large number of models that can reproduce the rare earth element (REE) spectrum of any single magma.

REEs were chosen because their behavior during melting processes produces smooth spectra on chondrite-normalized diagrams. These variations are directly related to their fractionation between minerals and silicate liquid during melting [36]. The spectra provide information on partial melting rates, with REE enrichment being inversely proportional to the melting rate [37].

Compared to primitive mantle magmas, the highly variable contents of MgO, Mg # (35.5 - 43.39) and transition elements (Ni, Cr, Co and Sc) in mafic hypovolcanic rocks suggest that some degree of fractional crystallization occurred during the emplacement of mafic hypovolcanic rocks [37]. This hypothesis is corroborated by the presence of spinel-rich magmas which suggests an ascent from depths greater than 30 km, at a significant speed not allowing the opportunity to react with the crust, and therefore to modify the composition of the magma [37].

In the diagrams of trace element variation as a function of La, Zr and Rb of the dolerites from the vicinity of Léré [38] (**Figure 7**), the La/Sm ratio tends to decrease with increasing La, which indicates fractional crystallization, while higher ratios are related to partial melting. The collinearities of trace element variations shown by the different diagrams (**Figure 7**) also indicate the probable development of fractional crystallization processes operating in more or less enriched and/or contaminated mantello-derived magmas. These processes would be more

developed for dolerites that could derive by fractional crystallization [39]. The correlation between the very incompatible elements (La and Nb) is linear and shows the existence of a genetic link between all these rocks (fractional crystallization or mixing of cogenetic magmas). This convention is verified by the fact that this line passes through the origin.

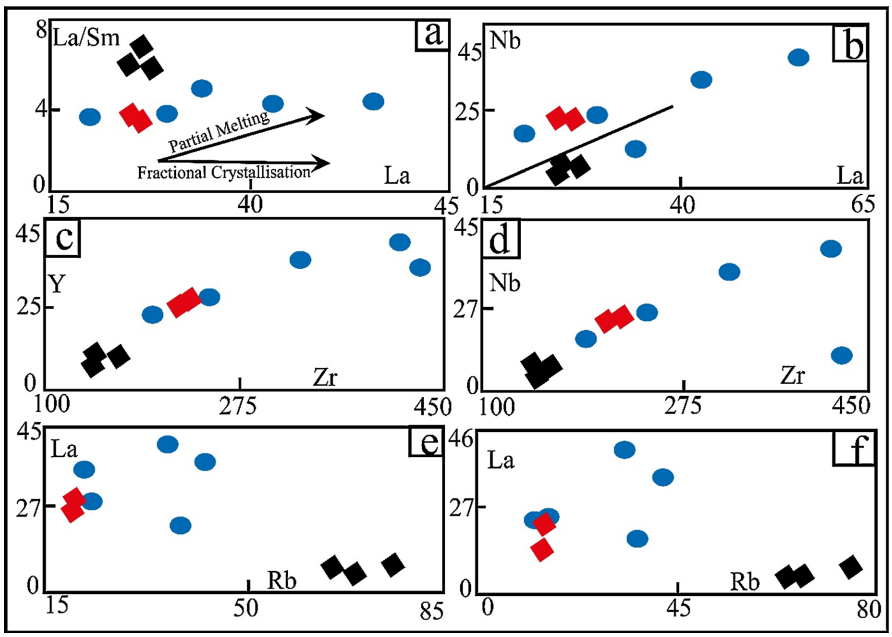

Figure 7. Diagram illustrating partial melting and fractional crystallization. Indicating the variation of trace elements as a function of La, Zr and Rb (a)-(f) in dolerites [38].

The fractional crystallization process was probably coupled with slight crustal contamination, as indicated by the Th/Yb enrichment of the studied dolerites. This has been observed in other continental tholeiites worldwide [1] [40]-[46]. The low content of transition elements refers to evolved parental magmas.

2) Source characterization

La bonne corrélation des éléments incompatibles LILE (Rb, Ba, K et Th) avec les éléments réputés immobiles comme les terres rares et le fait qu'ils ne suggèrent pas de corrélation avec la perte au feu (LOI) démontrent bien que la composition chimique des dolérites du socle panafricain n'est pas très affectée par les phénomènes secondaires d'altération et que leur richesse en ces éléments est une caractéristique primaire. High LREE contents are characteristic of alkaline magmas, whereas low concentrations are evident in tholeiitic magmas. The low TiO_2 content (1.28% - 3.44%) classifies the studied rocks in the continental tholeiite series with a low proportion of titanite oxides, such as that described in West Africa [47]. Dolerites with a low TiO_2 content would mainly result from the partial melting of a contaminated lithospheric mantle during subduction linked to the Pan-African orogeny of the chain [8]. Partial melting could therefore be associated with crustal contamination. The more or less high ratios (Zr/Hf: 35.09 - 45.82) of the studied dolerites compared to the primitive mantle (Zr/Hf: 36) demonstrate the participa-

tion of the metasomatized lithospheric mantle in the genesis of the studied rocks. The enrichment in LILE and LREE, characteristic of continental tholeiite, is interpreted either as the effect of a crustal contamination process [40] [48] [49], or as characteristic of the mantle source [50]-[52]. In the case of continental tholeiites in the study area, incompatible element ratios support their derivation from an enriched source such as enriched MORB (E-MORB) and OIB. High LREE contents are characteristic of alkaline magmas, while low contents are evidenced by tholeiitic magmas. Inferentially, alkaline rocks originate from a magma resulting from partial melting, unlike tholeiitic basalts. The studied dolerites are plotted in the ranges of uncontaminated lavas, further from the Pan-African basement granitoid domain. They appear to have a similar positive correlation to the uncontaminated lavas (**Figure 8(b)**).

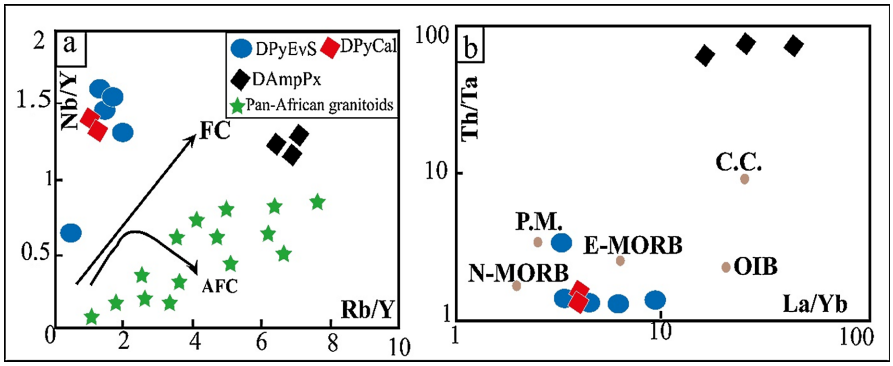

Figure 8. Diagrams illustrating the crustal contamination of the hypovolcanic rocks of Eastern Léré. (a) Nb/Y-Rb/Y diagram according to [49] and [55] showing the position of dolerites in relation to that of Pan-African granitoids. Data for Pan-African granitoids are from [20] [22] and [56]. CF: fractional crystallization; ACF: fractional assimilation-crystallization, (b) Position of the Figuil and Léré rocks in the Th/Ta vs La/Yb diagram [54]; OIB, E-MORB, N-MORB and PM according to Sun and [57], C. C: continental crust, according to Taylor and [58] crustal contamination, intraplate fractionation and fractional crystallization respectively according to Pearce.

3) Crustal contamination

The low content of transition elements refers to evolved parental magmas. The ratios (Y/Nb: 1.056 - 2.65) appear to characterize continental tholeiite. However, such a source is not clearly indicated in standardized HREE models. The different incompatible trace element ratios can be used to gain insight into the influence of the continental crust on magmatic composition. [53] demonstrated that crustal rocks and their derived fluids are characterized by high Rb/Nb ratios, whereas alkaline mafic magmas are enriched in Nb (hence, they will have a relatively low Rb/Nb ratio). The enrichment in LILE and LREE compared to enriched MORB (E-MORB) and OIB would result from the effect of crustal contamination [40] [48]. The analogy of the dolerites of the study area with the dolerites studied in other localities and the intervention of the crustal contamination process are also well illustrated by the Th/Ta vs La/Yb diagram of [54] (**Figure 8(b)**). The enrichment in LILE and LREE compared to enriched MORB (E-MORB) and OIB would

result from the effect of crustal contamination [49] [55]. The representative points of the rocks spread between the E-MORB and the OIB.

The studied dolerites are plotted in the ranges of uncontaminated lavas, further from the Pan-African basement granitoid domain. They appear to have a similar positive correlation to the uncontaminated lavas (**Figure 8(b)**).

4) Geodynamic context

In the Y/15-La/10-Nb/8 diagram (**Figure 9(a)**) of [27] the dolerites around Léré are located in two (2) domains namely: the pyrite and basement enclave dolerites and the pyrite and calcite dolerites are found in the late to post-orogenic intracontinental domain (compressive to distensive), except for a sample of pyrite and basement enclave dolerite facies which falls in the orogenic (compressive) domain; the amphibole and pyroxene dolerites are found in the orogenic (compressive) domain.

In the diagram (**Figure 9(b)**) TiO_2-MnO*10-P_2O_5*10 of [59], the majority of studied dolerites are found in the Oceanic Island Alkali Basalt (OIA) field, except for a sample of pyrite and basement enclave dolerites which are found in the Calc-Alkaline Basalt (CAB) field and the amphibole and pyroxene dolerites fall in the Island Arc Tholeiite (IAT) field. This diagram is used to differentiate the different magmatic series and geodynamic environments, *i.e.* it allows to place the magmatic series in the different geodynamic contexts.

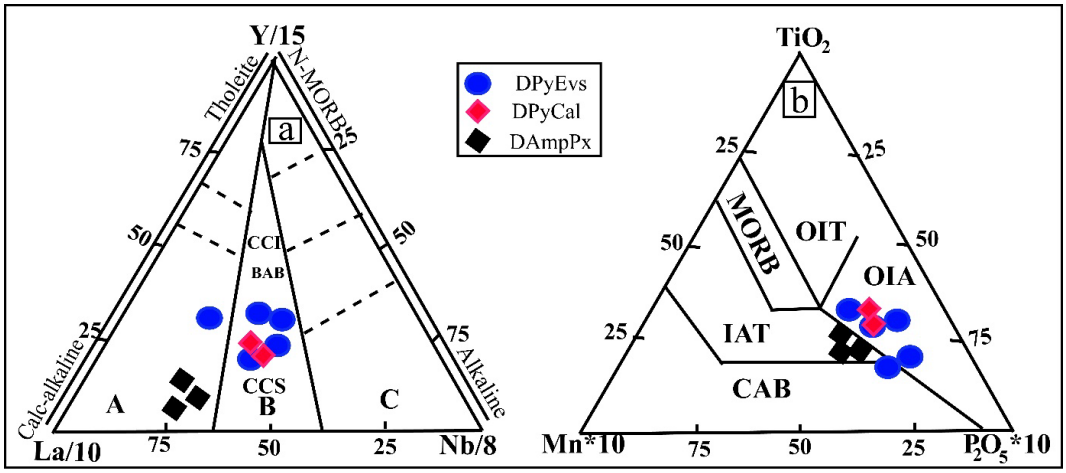

Figure 9. Diagrams illustrating the geodynamic context. (a) Diagram Y/15-La/10-Nb/8 of [27], BAB: back-arc basin basalts, CCI: lower continental crust, CCS: upper continental crust, A: orogenic domain (compressive), B: late to post-orogenic intracontinental domain (compressive to distensive), or intermediate domain of continental tholeiites (TC) and basin basalts back-arc (BAB), C: non-orogenic (distensive) domain of ridge tholeiites and intra-plate alkaline basalts. (b) Position of the East Léré rocks in Muller's TiO_2-MnO-P_2O_5 diagram [59], IOT: tholeiites from oceanic islands, OIA: alkaline basalts from oceanic islands, CAB: calc-alkaline basalts, IAT: island arc tholeiites and MORB: mid-oceanic ridge basalts.

The Zr/4-Y-2Nb diagram of [60] (**Figure 10**) shows that most of the dolerite samples studied are found in the intraplate alkali basalt zone. It is noteworthy that all amphibole and pyroxene dolerites are located outside the standard fields adequately defined by the diagram, including one sample of pyrite and enclave dolerite (BM2).

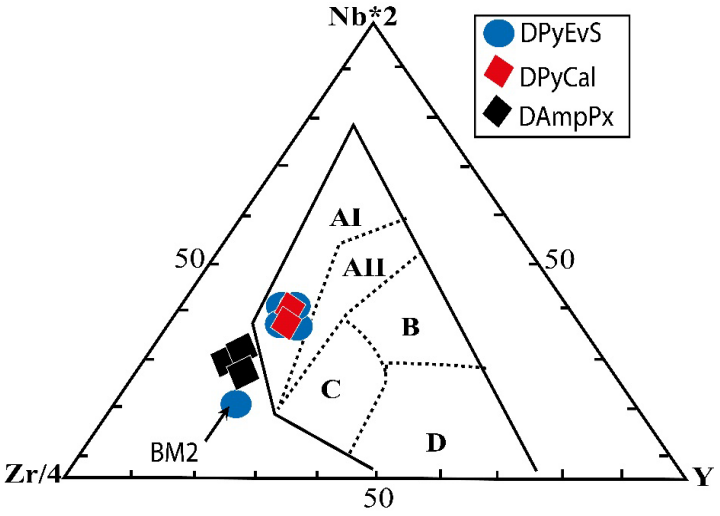

Figure 10. Zr/4-2Nb-Y tectonomagmatic diagram from Meschede [60] showing the geotectonic context of the mafic magmatic rocks of the eastern Léré basement. AI: intraplate alkaline basalts (WPA); AII: intraplate tholeiitic basalts (WPT); B: P-type mid-ocean ridge basalts (P-MORB), C: Volcanic arc basalts (VAB), D: N-type mid-ocean ridge basalts (N-MORB).

We can further note that the difference in the field distribution of these rocks does not necessarily suggest the emplacement of a distinct magmatic suite. Indeed, these variations may be due to differences in the emplacement environment. For example, injection into the Pan-African basement will be influenced, among other things, by the presence of fracture and fault networks, while injection into Cretaceous sedimentary basins may be favored by anisotropies linked to the presence of different stratigraphic contacts.

5. Conclusions

Field results show that the dolerite dykes around Léré, with widths ranging from 5 to 20 meters and lengths up to several kilometers, are oriented primarily E-W and N-S, with secondary directions SE-NW and N30E. These dolerites were emplaced as dykes across the Pan-African basement.

The structural features, combined with varied textures such as doleritic, intergranular granophyre, and ophitic, reflect the dynamic magmatic history and significant tectonic events that influenced the region. The presence of basement enclaves and minerals such as pyrite, calcite, and amphibole in the dolerites suggests magmatic contamination processes and interesting mineralogical potential.

For the rocks studied, the Al_2O_3, TiO_2 contents, and the fractionation of LREEs relative to HREEs, in addition to their differences in the geochemical diagrams used, all lead to the same results: the basic magmatic rocks studied are comparable to continental tholeiitic rocks generated in orogenic and intermediate contexts. The presence of continental tholeiites in Léré generally reflects a period of distension in this part of the Pan-African Range. This phase of continental extension would be contemporary with the oceanic opening in the Pan-African Range area.

The mode of emplacement of these doleritic intrusions of the Pan-African basement seems to be controlled by the major tectonic events that affected this study area. These dolerites, classified among the differentiated continental and oceanic tholeiites, were formed in a late- to post-orogenic (compressive to distensive) or compressive orogenic intracontinental geodynamic context.

These elements open promising perspectives for future studies, particularly regarding the magnetic characterization of the Léré dolerite dykes which could 1) determine pure multi-domain magnetite as the main mineral carrying magnetic susceptibility, 2) detect magnetic anomalies which will indicate the potential presence of mineral deposits and 3) understand how tectonic processes affected the formation and concentration of mineral resources. One can envisage, for the Léré magmatism, a process of fractional crystallization of a transitional basaltic magma, which would produce the basic to intermediate series, coupled with an assimilation of continental crust.

Conflicts of Interest

The authors declare no conflicts of interest regarding the publication of this paper.

References

[1] Srivastava, R.K. and Singh, R.K. (2004) Trace Element Geochemistry and Genesis of Precambrian Sub-Alkaline Mafic Dikes from the Central Indian Craton: Evidence for Mantle Metasomatism. *Journal of Asian Earth Sciences*, **23**, 373-389. https://doi.org/10.1016/s1367-9120(03)00150-0

[2] Coulon, C., Vidal, P., Dupuy, C., Baudin, P., Popoff, M., Maluski, H., *et al.* (1996) The Mesozoic to Early Cenozoic Magmatism of the Benue Trough (Nigeria); Geochemical Evidence for the Involvement of the St Helena Plume. *Journal of Petrology*, **37**, 1341-1358. https://doi.org/10.1093/petrology/37.6.1341

[3] Ngounouno, I., Déruelle, B., Guiraud, R. and Vicat, J. (2001) Magmatismes tholéiitique et alcalin des demi-grabens crétacés de Mayo Oulo-Léré et de Babouri-Figuil (Nord du Cameroun-Sud du Tchad) en domaine d'extension continentale. *Comptes Rendus de l'Académie des Sciences-Series IIA-Earth and Planetary Science*, **333**, 201-207. https://doi.org/10.1016/s1251-8050(01)01626-3

[4] Ernst, R.E. and Jowitt, S.M. (2013) Large Igneous Provinces (LIPs) and Metallogeny. Society of Economic Geologists Special Publication 17, 17-51.

[5] Ernst, R.E. and Buchan, K.L. (2002) Maximum Size and Distribution in Time and Space of Mantle Plumes: Evidence from Large Igneous Provinces. *Journal of Geodynamics*, **34**, 309-342. https://doi.org/10.1016/s0264-3707(02)00025-x

[6] Hargitai, H., Kereszturi, Á., Cornet, T. and Illés-Almár, E. (2014) Large Igneous Province. In: Hargitai, H. and Kereszturi, Á., Eds., *Encyclopedia of Planetary Landforms*, Springer, 1-9. https://doi.org/10.1007/978-1-4614-9213-9_215-1

[7] Toteu, S.F. (1987) Chronologie des grands ensembles structuraux de la région de Poli. Accrétion crustale dans la chaine panafricaine du Nord-Cameroun. Thèse de Doctorat d'Etat, Univ. de Nancy, inédite, 197 p.

[8] Toteu, S.F. (1990) Geochemical Characterization of the Main Petrographical and Structural Units of Northern Cameroon: Implications for Pan-African Evolution. *Journal of African Earth Sciences* (*and the Middle East*), **10**, 615-624.

https://doi.org/10.1016/0899-5362(90)90028-d

[9] Vicat, J. and Vellutini, P. (1987) Sur la nature et la signification des dolerites du bassin precambrien de sembe-ouesso (republique du congo). *Precambrian Research*, **37**, 57-69. https://doi.org/10.1016/0301-9268(87)90039-8

[10] Ekwueme, B.N. (1994) Basaltic Magmatism Related to the Early Stages of Rifting along the Benue Trough: The Obudu Dolerites of Southeast Nigeria. *Geological Journal*, **29**, 269-276. https://doi.org/10.1002/gj.3350290306

[11] Klamadji, M.N., Dedzo, M.G., Tchameni, R. and Dawaï, D. (2020) Petrography and Geochemical Characterization of Dolerites from Figuil (Northern Cameroon) and Léré (Southwestern Chad). *International Journal of Geosciences*, **11**, 459-482. https://doi.org/10.4236/ijg.2020.117023

[12] Klamadji, M.N., Dedzo, M.G., Tchameni, R., Hamadjoda, D.D., Nyotok, P.C.B.à. and Onana, G. (2021) Fractional Crystallization and Crustal Contamination of Doleritic and Trachytic Dykes Crosscutting the Cretaceous Sedimentary Basins from Figuil (North Cameroon) and Léré (South-Western Chad): Geodynamic Implications. *Journal of Geoscience and Environment Protection*, **9**, 190-210. https://doi.org/10.4236/gep.2021.912012

[13] Ngarena, K.M., Léotine, T., Gustave, B.R., Dedzo, M.G., Felix, D.N., Felix, B.L., *et al.* (2025) Geochemical Characterizations of the Hypovolcanic Formations of the Pan-African Basement and the Cretaceous Sedimentary Basins of Figuil (North Cameroon) and Léré (Southwest Chad): Petrogenetic and Geodynamic Implication of the Pan-African Range of Central Africa (CPAC). *International Journal of Geosciences*, **16**, 127-153. https://doi.org/10.4236/ijg.2025.162007

[14] Jean-Claude, D.M., *et al.* (2025) The Dolerites of the Léré Region (Southwestern Chad, Africa): Petrography and Geochemical Characterisation. *International Journal of Multidisciplinary Research and Publications*, **7**, 22-32.

[15] Bessoles, B. (1980) Géologie de l'Afrique, la chaine panafricaine "zone mobile d'Afrique centrale (partie sud) et zone mobile soudanaise": Géologie de l'Afrique, la chaine panafricaine "zone mobile d'Afrique centrale (partie sud) et zone mobile soudanaise".

[16] Theunissen, K., Lenoir, J.-L., Liégois, J.-P., Delvaux, D. and Mruma, A. (1992) Empreinte pan-africaine majeure dans la chaîne ubendienne de Tanzanie sud-occidentale: Géochronologie U-Pb sur zircon et contexte structural. *Comptes Rendu de l'Académie des Sciences de Paris*, **314**, 1355-1362.

[17] Caby, R., Bertrand, J.M.L. and Black, R. (1981) Chapter 16. Pan-African Ocean Closure and Continental Collision in the Hoggar-Iforas Segment, Central Sahara. In: *Developments in Precambrian Geology*, Elsevier, 407-434. https://doi.org/10.1016/s0166-2635(08)70021-5

[18] Teixeira, W. and Figueiredo, M.C.H. (1991) An Outline of Early Proterozoic Crustal Evolution in the São Francisco Craton, Brazil: A Review. *Precambrian Research*, **53**, 1-22. https://doi.org/10.1016/0301-9268(91)90003-s

[19] Kasser, M.Y. (1995) Evolution précambrienne de la région du Mayo-Kebbi. Un segment de la Chaîne Panafricaine. Thèse Muséum National d'Histoire Naturelle de Paris, 217 p.

[20] Doumnang Mbaigane, J.-C. (2006) Géologie des formations Néoprotérozoïque du Mayo Kebbi (Sud-Ouest du Tchad): Apport de la pétrologie et de la géochimie: Implications sur la géodynamique au Panafricain. These de doctorat, Orléans.

[21] Pouclet, A., Vidal, M., Doumnang, J., Vicat, J. and Tchameni, R. (2006) Neoproterozoic Crustal Evolution in Southern Chad: Pan-African Ocean Basin Closing, Arc Accretion and Late- to Post-Orogenic Granitic Intrusion. *Journal of African Earth*

Sciences, **44**, 543-560. https://doi.org/10.1016/j.jafrearsci.2005.11.019

[22] Isseini, M. (2011) Croissance et différenciation crustales au Néoprotérozoïque: Exemple du domaine panafricain du Mayo Kebbi au Sud-Ouest du Tchad. PhD Thesis, Université Henri Poincaré-Nancy 1.

[23] Mbaguedje, D. (2015) Métallogénie de l'or et de l'uranium dans le cadre de la croissance et de la différenciation de la croûte au Néoprotérozoïque: exemple du massif du Mayo-Kebbi (Tchad) dans la Ceinture Orogénique d'Afrique Centrale. PhD Thesis, Université de Lorraine.

[24] Penaye, J., Kröner, A., Toteu, S.F., Van Schmus, W.R. and Doumnang, J. (2006) Evolution of the Mayo Kebbi Region as Revealed by Zircon Dating: An Early (ca. 740 Ma) Pan-African Magmatic Arc in Southwestern Chad. *Journal of African Earth Sciences*, **44**, 530-542. https://doi.org/10.1016/j.jafrearsci.2005.11.018

[25] Schwoerer, P. (1965) Carte géologique de reconnaissance à l'échelle du 1/500 000 et Notice explicative sur la feuille Garoua-Est. Dir. Mines Géol., 49 p.

[26] Wager, L.R. and Deer, W.A. (1939) Olivines from the Skaergaard intrusion, Kangerdlugssuak, East Greenland. *American Mineralogist*, **24**, 18-25.

[27] Cabanis, B. and Lecolle, M. (1989) Le diagramme La/10-Y/15-Nb/8: Un outil pour la discrimination des séries volcaniques et la mise en évidence des processus de mélange et/ou de contamination crustale. *Comptes rendus de l'Académie des Sciences Paris*, **309**, 2023-2029.

[28] Le Maître, R.W. (2002) Igneous Rocks. A Classification and Glossary of Terms. Recommendations of the International Union of Geological Sciences Sub Commission on the Systematics of Igneous Rocks. Cambridge Univ. Press.

[29] Irvine, T.N. and Baragar, W.R.A. (1971) A Guide to the Chemical Classification of the Common Volcanic Rocks. *Canadian Journal of Earth Sciences*, **8**, 523-548. https://doi.org/10.1139/e71-055

[30] McDonough, W.F. and Sun, S.-. (1995) The Composition of the Earth. *Chemical Geology*, **120**, 223-253. https://doi.org/10.1016/0009-2541(94)00140-4

[31] Tchouankoue, J.P., Wambo, N.A.S., Dongmo, A.K. and Wörner, G. (2012) Petrology, Geochemistry, and Geodynamic Implications of Basaltic Dyke Swarms from the Southern Continental Part of the Cameroon Volcanic Line, Central Africa. *The Open Geology Journal*, **6**, 72-84. https://doi.org/10.2174/1874262901206010072

[32] Nkouandou, O., Aminatou, M., Iancu, G. and Bardintzeff, J.-M. (2015) Petrology and Geochemistry of Doleritic Dyke of Likok (Cameroon, Central Africa). *Carpathian Journal of Earth and Environmental Sciences*, **10**, 121-132.

[33] Campbell, I.H. (1985) The Difference between Oceanic and Continental Tholeiites: A Fluid Dynamic Explanation. *Contributions to Mineralogy and Petrology*, **91**, 37-43. https://doi.org/10.1007/bf00429425

[34] Vicat, J., Ngounouno, I. and Pouclet, A. (2001) Existence de dykes doléritiques anciens à composition de tholéiites continentales au sein de la province alcaline de la ligne du Cameroun. Implication sur le contexte géodynamique. *Comptes Rendus de l'Académie des Sciences-Series IIA-Earth and Planetary Science*, **332**, 243-249. https://doi.org/10.1016/s1251-8050(01)01526-9

[35] Chamboredon, R. (2015) Caractérisation et origine des magmas alcalins et des fluides sous le massif volcanique du Jbel Saghro, Anti Atlas, Maroc. Thèse de Doctorat, Univ. De Montpellier, 173 p.

[36] Shaw, D.M. (1970) Trace Element Fractionation during Anatexis. *Geochimica et Cosmochimica Acta*, **34**, 237-243. https://doi.org/10.1016/0016-7037(70)90009-8

[37] Frey, F.A., Green, D.H. and Roy, S.D. (1978) Integrated Models of Basalt Petrogenesis: A Study of Quartz Tholeiites to Olivine Melilitites from South Eastern Australia Utilizing Geochemical and Experimental Petrological Data. *Journal of Petrology*, **19**, 463-513. https://doi.org/10.1093/petrology/19.3.463

[38] Bendoukha, R. (2008) Etude dynamique, pétrographique et géochimique du volcanisme alcalin plio-quaternaire de l'Oranie (Algérie nord occidentale). Alger.

[39] Ikenne, M., Mortaji, A., Gasquet, D. and Stussi, J.M. (1997) Les filons basiques des boutonnières du Bas Drâa et de la Tagragra d'Akka: Témoins des distensions néoprotérozoïques de l'Anti-Atlas occidental (Maroc). *Journal of African Earth Sciences*, **25**, 209-223. https://doi.org/10.1016/s0899-5362(97)00099-7

[40] Dupuy, C. and Dostal, J. (1984) Trace Element Geochemistry of Some Continental Tholeiites. *Earth and Planetary Science Letters*, **67**, 61-69. https://doi.org/10.1016/0012-821x(84)90038-4

[41] Marsh, J.S. (1989) Geochemical Constraints on Coupled Assimilation and Fractional Crystallization Involving Upper Crustal Compositions and Continental Tholeiitic Magma. *Earth and Planetary Science Letters*, **92**, 70-80. https://doi.org/10.1016/0012-821x(89)90021-6

[42] Valbracht, P.J., Helmers, H. and Beunk, F.F. (1991) Early Proterozoic Continental Tholeiites from Western Bergslagen, Central Sweden, I. Petrology, Geochemical Petrogenesis and Geotectonic Setting. *Precambrian Research*, **52**, 187-214. https://doi.org/10.1016/0301-9268(91)90080-t

[43] Tembo, F., Kampunzu, A.B. and Porada, H. (1999) Tholeiitic Magmatism Associated with Continental Rifting in the Lufilian Fold Belt of Zambia. *Journal of African Earth Sciences*, **28**, 403-425. https://doi.org/10.1016/s0899-5362(99)00012-3

[44] Cadman, A.C., Tarney, J., Bridgwater, D., Mengel, F., Whitehouse, M.J. and Windley, B.F. (2001) The Petrogenesis of the Kangâmiut Dyke Swarm, W. Greenland. *Precambrian Research*, **105**, 183-203. https://doi.org/10.1016/s0301-9268(00)00111-x

[45] Ingle, J.C., Karig, D.E. and Moore, T.C. (2004) Calcium Carbonate Analysis of Hole 31-296 [Dataset]. PANGAEA. https://doi.org/10.1594/PANGAEA.223545

[46] Worthing, M.A. (2005) Petrology and Geochronology of a Neoproterozoic Dyke Swarm from Marbat, South Oman. *Journal of African Earth Sciences*, **41**, 248-265. https://doi.org/10.1016/j.jafrearsci.2005.04.003

[47] Marzoli, A., Bertrand, H., Knight, K.B., Cirilli, S., Buratti, N., Vérati, C., *et al.* (2004) Synchrony of the Central Atlantic Magmatic Province and the Triassic-Jurassic Boundary Climatic and Biotic Crisis. *Geology*, **32**, Article No. 973. https://doi.org/10.1130/g20652.1

[48] Dostal, J., Baragar, W.R.A. and Dupuy, C. (1983) Geochemistry and Petrogenesis of Basaltic Rocks from Coppermine River Area, Northwest Territories. *Canadian Journal of Earth Sciences*, **20**, 684-698. https://doi.org/10.1139/e83-062

[49] Cox, K.G. and Hawkesworth, C.J. (1985) Relative Contribution of Crust and Mantle to Flood Basalt Magmatism, Mahabaleshwar, Deccan Traps. *Philosophic Transaction Royal Society London A*, **310**, 627-641.

[50] Bertrand, H., Dostal, J. and Dupuy, C. (1982) Geochemistry of Early Mesozoic Tholeiites from Morocco. *Earth and Planetary Science Letters*, **58**, 225-239. https://doi.org/10.1016/0012-821x(82)90196-0

[51] Alibert, C. (1985) A Sr-Nd Isotope and REE Study of Late Triassic Dolerites from the Pyrenees (France) and the Messejana Dyke (Spain and Portugal). *Earth and Planetary Science Letters*, **73**, 81-90. https://doi.org/10.1016/0012-821x(85)90036-6

[52] Bertrand, H. (1991) The Mesozoic Tholeiitic Province of Northwest Africa: A Volcano-Tectonic Record of the Early Opening of Central Atlantic. In: Kampunzu, A.B. and Lubala, R.T., Eds., *Magmatism in Extensional Structural Settings*, Springer, 147-188. https://doi.org/10.1007/978-3-642-73966-8_7

[53] Weaver, B.L. and Tarney, J. (1984) Empirical Approach to Estimating the Composition of the Continental Crust. *Nature*, **310**, 575-577. https://doi.org/10.1038/310575a0

[54] Condie, K.C. (1997) Sources of Proterozoic Mafic Dyke Swarms: Constraints from Thta and Layb Ratios. *Precambrian Research*, **81**, 3-14. https://doi.org/10.1016/s0301-9268(96)00020-4

[55] Leeman, W.P. and Hawkesworth, C.J. (1986) Open Magma Systems: Trace Element and Isotopic Constraints. *Journal of Geophysical Research*: *Solid Earth*, **91**, 5901-5912. https://doi.org/10.1029/jb091ib06p05901

[56] Nlomngan, J.P.S., Penaye, J., Tchameni, R., Owona, S., Ibohn, A.P.M., Nsifa, E.N., *et al.* (2019) Geochemical Characterization of Boula Ibi Granitoids and Implications in Geodynamic Evolution. *Journal of Geography and Geology*, **11**, 13-28. https://doi.org/10.5539/jgg.v11n4p13

[57] Sun, S. and McDonough, W.F. (1989) Chemical and Isotopic Systematics of Oceanic Basalts: Implications for Mantle Composition and Processes. In: Saunders, A.D. and Norry, M.J., Eds., *Magmatism in the Ocean Basins*, Geological Society, London, Special Publications, No. 42, 313-345. https://doi.org/10.1144/gsl.sp.1989.042.01.19

[58] Taylor, S.R. and McLennan, S.M. (1985) The Continental Crust: It's Composition and Evolution. Blackwell, 312 p.

[59] Muller (1983) MnO-TiO_2-P_2O_5 Discrimination Diagram for Basaltic Rocks (45-54 wt.% SiO_2) from the Porten Road, Eel River, and Oak Mountain Formations.

[60] Meschede, M. (1986) A Method of Discriminating between Different Types of Mid-Ocean Ridge Basalts and Continental Tholeiites with the Nb-Zr-Y Diagram. *Chemical Geology*, **56**, 207-218. https://doi.org/10.1016/0009-2541(86)90004-5